Acta Pharmaceutica Sinica B 2025;15(4):1956−1973

Chinese Pharmaceutical Association
Institute of Materia Medica, Chinese Academy of Medical Sciences

Acta Pharmaceutica Sinica B

www.elsevier.com/locate/apsb
www.sciencedirect.com

ORIGINAL ARTICLE

GRK2 activates TRAF2−NF-κB signalling to promote hyperproliferation of fibroblast-like synoviocytes in rheumatoid arthritis

Chenchen Han[a,†], Liping Jiang[a,†], Weikang Wang[a,†], Shujun Zuo[a], Jintao Gu[a], Luying Chen[a], Zhuo Chen[a], Jiajie Kuai[a], Xuezhi Yang[a], Liang Xu[b,*], Yang Ma[a,*], Wei Wei[a,*]

[a]*Institute of Clinical Pharmacology, Anhui Medical University, Key Laboratory of Anti-inflammatory and Immune Medicine, Ministry of Education, Anhui Collaborative Innovation Center of Anti-inflammatory and Immune Medicine, Hefei 230032, China*
[b]*Orthopedic Department, First Affiliated Hospital of the University of Science and Technology of China (USTC), Anhui Provincial Hospital, Hefei 230002, China*

Received 23 September 2024; received in revised form 17 December 2024; accepted 18 February 2025

KEY WORDS

Rheumatoid arthritis;
Fibroblast-like synoviocytes;
Hyperproliferation;
G protein-coupled receptor kinase 2;
Tumor necrosis factor receptor-associated factor 2

Abstract G protein-coupled receptor kinase 2 (GRK2) participates in the phosphorylation and desensitization of G protein-coupled receptor (GPCR), impacting various biological processes such as inflammation and cell proliferation. Dysregulated expression and activity of GRK2 have been reported in multiple cells in rheumatoid arthritis (RA). However, whether and how GRK2 regulates synovial hyperplasia and fibroblast-like synoviocytes (FLSs) proliferation is poorly understood. In this study, we investigated the regulation of GRK2 and its biological function in RA. We found that GRK2 transmembrane activity was increased in FLSs of RA patients and collagen-induced arthritis (CIA) rats. Additionally, we noted a positive correlation between high GRK2 expression on the cell membrane and serological markers associated with RA and CIA. Immunoprecipitation−mass spectrometry and pull-down analyses revealed tumor necrosis factor receptor-associated factor 2 (TRAF2) as a novel substrate of GRK2. Furthermore, surface plasmon resonance (SPR) and molecular docking assays determined that the C-terminus of GRK2 binds to the C-terminus of TRAF2 at the Gln340 residue. GRK2 knockdown and the GRK2 inhibitor CP-25 attenuated synovial hyperplasia and FLS proliferation in CIA both *in vitro* and *in vivo* by decreasing GRK2 membrane expression and activity. Mechanistically, increased GRK2 transmembrane activity contributed to the recruitment of TRAF2 on the cell membrane, promoting GRK2

*Corresponding authors.
E-mail addresses: wwei@ahmu.edu.cn (Wei Wei), mayang_ahmu@126.com (Yang Ma), salxuliang@ustc.edu.cn (Liang Xu).
[†]These authors made equal contributions to this work.
Peer review under the responsibility of Chinese Pharmaceutical Association and Institute of Materia Medica, Chinese Academy of Medical Sciences.

https://doi.org/10.1016/j.apsb.2025.02.031

−TRAF2 interactions that facilitate the recruitment of the E3 ubiquitin ligase TRIM47 to TRAF2. This enhanced TRAF2 Lys63 polyubiquitylation and induced nuclear factor (NF)-κB activation, leading to synovial hyperplasia and abnormal proliferation of FLSs. Our study provides a mechanistic and preclinical rationale for further evaluation of GRK2 as a therapeutic target for RA.

1. Introduction

Rheumatoid arthritis (RA) is a prevalent chronic autoimmune disease and is typically marked by ongoing synovial inflammation, synovium hyperplasia, and aggressive pannus formation, which contributes to the destruction of cartilage and bone[1]. Numerous studies have gradually revealed that fibroblast-like synoviocytes (FLSs), as key resident cells in the synovial lining, actively participate in and exacerbate the process of cartilage injury by secreting a series of pro-inflammatory cytokines, such as tumor necrosis faction-α (TNF-α), interleukin-1β (IL-1β), IL-6, and prostaglandin E2 (PGE2). They play a central role in the pathogenesis of RA[2-7]. Identifying the pivotal molecules driving these pro-inflammatory cytokine-mediated signalling pathways may clarify the mechanisms resulting in abnormal proliferation and activation of FLSs, which may uncover novel molecular targets for precision therapies to treat RA.

G-protein-coupled receptor kinase 2 (GRK2) belongs to the serine/threonine kinase family and plays an integral role in regulating key biological processes such as phosphorylation, desensitization and internalization of G-protein-coupled receptors (GPCR). Consequently, GRK2 is essential for various biological processes, including cell proliferation and inflammation[8-11]. GRK2 is characterized by three important sequence features. The N-terminus includes a conserved segment that forms an αN helix in the active state of GRK2, which is succeeded by the initial eight helices of the regulatory G-protein signaling homology (RH) domain[12,13]. Secondly, the kinase domain consists of a nine-helix bundle that is situated within a loop connecting helices 8 and 9 of the RH domain. This kinase domain features critical amino acid residues, such as Lys220, which is essential for determining kinase activity[14,15]. Lastly, the C-terminal domains of GRK2, which are less conserved, follow the kinase domain. This C-terminus of GRK2 binds to multiple proteins, such as GPCR, phosphatidylinositol 3-kinase (PI3K), and protein kinase B (AKT). Importantly, phosphorylation at Ser685 within the C-terminus of GRK2 plays a crucial role in facilitating the recruitment of GRK2 to the cell membrane[16-18].

Our previous work demonstrated that increased GRK2 translocation plays a specific role in improving arthritis and that the binding of GRK2 to extracellular signal-regulated kinase (ERK1/2), Salvador homolog-1 (SAV1), peroxisome proliferator-activated receptor gamma (PPARγ), or prostaglandin receptor 4 (EP4) leads to the dysfunction of FLSs, endothelial cells, and immune cells. Additionally, the GRK2 inhibitor CP-25 has been shown to effectively suppress the abnormal proliferation and excessive migration of FLSs[19-26]. Despite progress, the underlying mechanisms linking GRK2 to FLS hyperproliferation remain incompletely understood.

In this study, we demonstrate that GRK2 facilitates the recruitment of TRAF2 to the cell membrane, promoting the formation of the TRAF2−tripartite motif-containing (TRIM) 47 complex. This interaction mediates the Lys63 polyubiquitylation of TRAF2 and activates NF-κB signalling in FLSs, contributing to RA progression. Together, our findings report a novel role for GRK2 in the development of RA and highlight the GRK2−TRAF2−NF-κB pathway as a promising therapeutic target to mitigate FLS hyperproliferation in RA.

2. Materials and methods

2.1. Patients and specimens

RA blood samples were obtained from patients diagnosed with RA[27], and control blood samples were sourced from individuals without a history of RA undergoing lower limb amputation owing to traffic accidents and healthy controls. RA synovial tissue (ST) was obtained from RA patients who received surgical synovectomy of the knee, while normal ST was collected from donors without a history of RA who underwent arthroscopic surgery after traumatic fractures. This study obtained official ethical approval (approval No. 2020KY74) from the Biomedical Ethics Review Committee of the First Affiliated Hospital of the University of Science and Technology of China (Hefei). In addition, all patients participating in the study have given clear informed consent after fully understanding the research content. Detailed clinical characteristics are presented in Supporting Information Table S1. Notably, there was no involvement of patients or the public in the study's design, execution, reporting, or dissemination plans.

2.2. Animals

This experiment used 6−8 week-old Wistar rats provided by Beijing Vital River Laboratory Animal Technology Co., Ltd. (SYXK(Wan)-2020-001), whose body weight ranged from approximately 150 ± 20 g. The rats were housed in a specific pathogen-free environment of Anhui Medical University, with controlled room temperature set between 20 and 22 °C and humidity maintained at 40%−60%. The study received ethical approval from the Ethics Review Committee for Animal Experimentation of Anhui Medical University, Hefei, China (approval No. 20201002).

2.3. Cells and reagents

Human embryonic kidney (HEK293) and RA FLS cell lines (MH7A) were sourced from Beijing Jinheng Shengshi Technology Co., Ltd. PGE2 (Cayman Chemical, cat. 14010), recombinant rat TNF-α (Novoprotein, cat. CR38, purity >95%), recombinant human TNF-α (Novoprotein, cat. C008, purity >95%), and etanercept (dimeric fusion protein) were procured from TargetMol and Shanghai Guojian Pharmaceutical Enterprise Co., Ltd.,

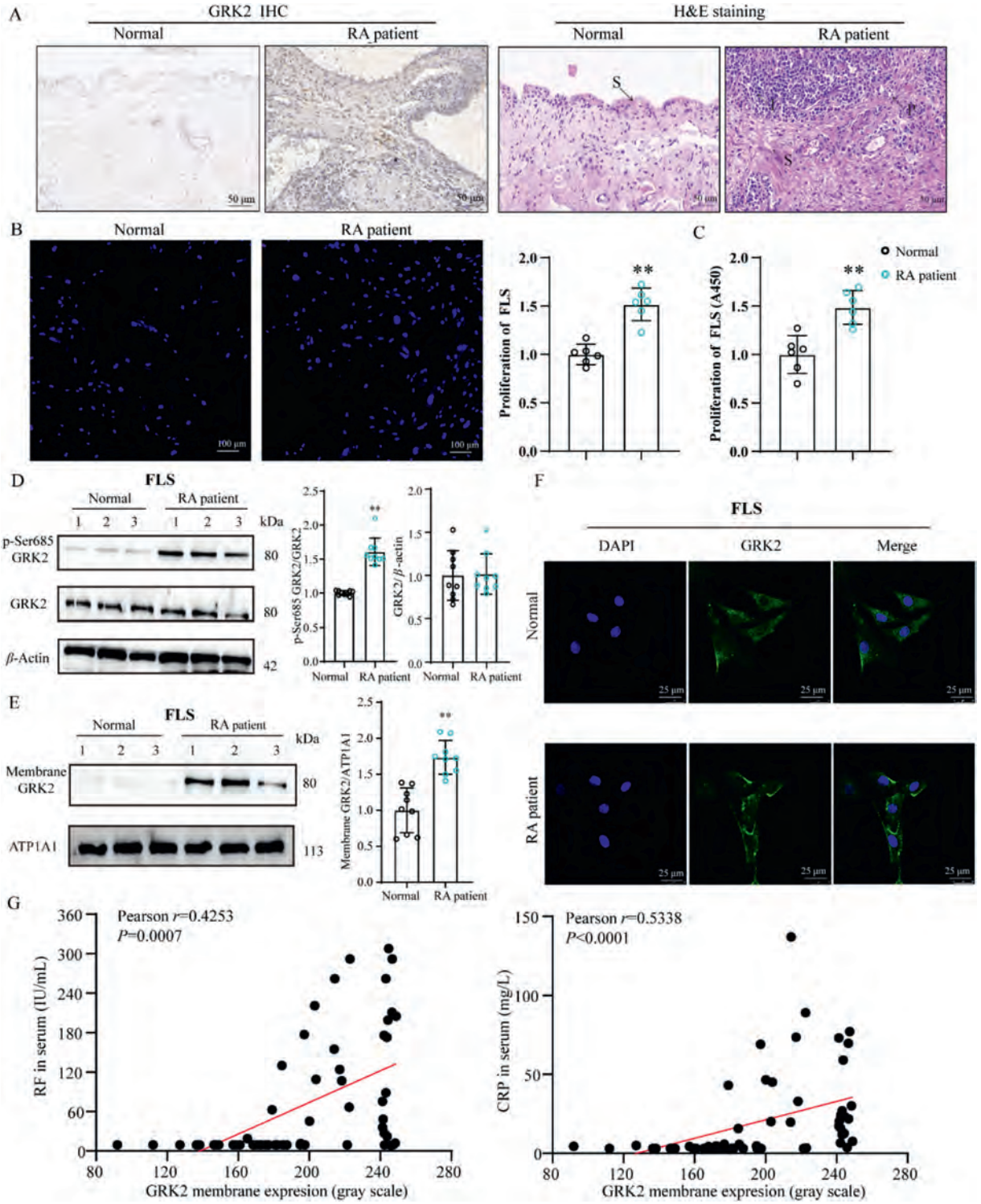

Figure 1 Membrane expression of GRK2 in FLSs of RA patients. (A) IHC staining of GRK2 expression in the joint synovium of healthy donors and patients with RA ($n = 6$, scale bar = 50 μm). (B) Images were captured with a high-content cell imager and the number of cells was counted ($n = 6$, scale bar = 100 μm, Student's *t*-test, $^{**}P < 0.01$ *vs*. normal group). (C) CCK-8 was used to detect cell proliferation activity ($n = 6$, Student's *t*-test, $^{**}P < 0.01$ *vs*. normal group). (D) *p*-Ser685 GRK2 and GRK2 protein levels in FLSs of RA were detected by Western blot ($n = 9$, Student's *t*-test, $^{**}P < 0.01$ *vs*. normal group). (E) GRK2 membrane expression in FLSs of RA was detected by membrane protein extraction kit and Western blot ($n = 9$, Student's *t*-test, $^{**}P < 0.01$ *vs*. normal group). (F) GRK2 intracellular localization in FLSs of RA was detected by confocal microscope ($n = 5$, scale bar = 25 μm). (G) Correlation analysis of GRK2 membrane expression of healthy donors and patients with RA with RF ($n = 30$, Pearson coefficient analysis, $r = 0.4253$, $P = 0.0007$) and CRP ($n = 30$, Pearson coefficient analysis, $r = 0.5338$, $P < 0.0001$). All data are presented as mean ± SD.

GRK2 activity inhibitor CP-25 was supplied by the Institute of Clinical Pharmacology, Anhui Medical University (Hefei, China). Dimethyl sulfoxide (DMSO) was sourced from Sigma−Aldrich, and Chicken Collagen Type II (CCII) (cat. 20012) and complete Freund's adjuvant (CFA) (cat. 7001) were supplied by Chondrex. Enzyme-linked immunosorbent assay (ELISA) kits for various cytokines including PGE2, TNF-α, IL-6, IL-1β, IL-17a, interferon γ (IFN-γ), IL-4, IL-10, and transforming growth factor β (TGF-β) were provided by Beijing Furui Runze Biotechnology Co., Ltd. Membrane protein extraction kit was purchased from Bestbio. Protein A/G binding agarose beads (cat. sc-2003) were purchased from Santa Cruz Biotechnology. DAPI (cat. C1005) was sourced from Beyotime. PlasMem Bright Red (cat. P505) was purchased from DOJINDO. Human GRK2 protein (His Tag) and Human TRAF2 protein (His Tag) were acquired from Tsingke Biotechnology Co., Ltd.

2.4. Plasmids and antibodies

In this study, various tagged constructs of TRAF2 and GRK2 were used. Plasmids with FLAG-tag were created by inserting the relevant cDNAs into the pcDNA-3.1(+) vector. Similarly, plasmids with MYC-tag were formed by subcloning the relevant cDNAs into the pcDNA-3.1(+) vector. The plasmids employed in this research were developed in our laboratory and were purchased from General Biol (Anhui) Co., Ltd., including FLAG-TRAF2-WT, FLAG-TRAF2-ΔC (amino acids 1−272), MYC-GRK2-WT, MYC-GRK2-ΔC (amino acids 1−513), EGFP-TRAF2-Gln340Arg, pcDNA3.1-FLAG, -MYC, and -EGFP.

Antibodies: TRAF2 from Santa Cruz Biotechnology (cat. sc-136999) and Cell Signaling Technology (cat. 4712; GRK2 from Huabio (cat. ET1609-72) and Santa Cruz Biotechnology (cat. sc-13143); TRIM47 from Proteintech (cat. 26885-1-AP), FLAG from Affinity Biosciences (cat. T003) and Cell Signaling Technology (cat. 14793); C-Myc-Tag from Affinity Biosciences (cat. T001) and Cell Signaling Technology (cat. 2278); p-P65 from Cell Signaling Technology (cat. 3033), P65 from Cell Signaling Technology (cat. 8242); K63-linkage specific polyubiquitin antibodies from Cell Signaling Technology (cat. 5621), p-Ser685 GRK2 from CUSABIO (cat. CSB-PA007551) and Sigma−Aldrich (cat. SAB4504682), ATP1alpha1/Na^+K^+ATPase1 (ATP1A1) from HUABIO (cat. ET1609-76); Histone-H3 from Proteintech (cat. 17168-1-AP); β-actin from ZSGB-BIO (cat. TA-09). Alexa-Fluor-488 tagged secondary antibodies were sourced from Proteintech (cat. srbAF488-1).

2.5. Collagen-induced arthritis (CIA) model of rats

CCII was effectively dissolved in a 0.01 mol/L acetic acid (4 mg/mL), and then mixed with an equal volume of CFA (4 mg/mL) to create a homogeneous emulsion. On Day 0, rats received intradermal injections of 0.1 mL of this emulsion at various sites, including the base of the tail, the back, and the right hind limb. On Day 7, the Wistar rats were re-injected intradermally with another 0.1 mL of the CCII emulsion at multiple locations on the tail or back. By Day 14, secondary joint swelling was observed, confirming a 98% success rate for the CIA model, with unsuccessful models being excluded from further analysis.

To identify the role of GRK2, recombinant adeno-associated virus 5 (AAV5) with or without *Grk2* knockdown (20 μL, 1×10^{12} vg/mL) was injected into the intra-articular cavity of CIA Wistar rats for 3 weeks, namely CIA + AAV5-*Grk2*-shRNA and CIA + AAV5-NC group, each group with 6 rats. Lentiviral shRNA targeting *Grk2* was purchased from Genomeditech. The shRNA oligos were as follows: NC: 5′-TTCTCCGAACGTGTCACGT-3′; *Grk2*-shRNA1: 5′-GGGATGTGTTCCACAAGTTCA-3′; *Grk2*-shRNA2: 5′-GCATCATGCATGGCTACATGT-3′; *Grk2*-shRNA3: 5′-GGTCTATGGGTGCCGGAA-AGC-3′. Cells were transfected with lentiviral *Grk2* shRNA oligos or the corresponding plasmids using jetPRIME (Polyplus, 101000046), following the guidelines. Analysis of the cells was conducted 36−48 h after transfection.

Grouping: a vehicle-treated CIA group, a group treated with CP-25 [50 mg/kg/day, Intragastric administration (i.g.)] for three weeks, and a group receiving etanercept [3 mg/kg/3 days, hypodermic injection (i.h.)] for the same duration, with each group consisting of six rats. Body weight, swollen joint count, arthritis index, global assessment, and secondary paw swelling were evaluated according to the principle of randomized controlled trials. On Day 35, the rats were euthanized to analyse blood, spleens, ST, and joint change.

2.6. FLSs proliferation assay (High-Content Imaging System)

The cell suspension obtained after-digestion was placed into a 96-well plate (5×10^4 cells/well). After overnight culture in 5% FBS, the cells were treated with PGE2, TNF-α, CP-25, or etanercept for 24 h. After treatment, cells were fixed with 4% formaldehyde, and stained using DAPI. High-Content Imaging System with ImageXpress Micro-4 captured cell images to count cell number (Molecular Devices LLC., USA).

2.7. FLSs proliferation assay (CCK-8 assay)

Cell suspension (5×10^5 cells/mL, 100 μL/well) was added to a 96-well plate and incubated for 24 h with different stimulation. Then, CCK-8 (10 μL/well) was introduced and incubated for 3 h. After incubation, a microplate reader with Infinite M1000 PRO system (Tecan, Switzerland) measured the absorbance of cells at 450 nm.

2.8. Haematoxylin and eosin (H&E) staining

ST, knee and ankle joints samples were treated with paraffin embedding followed by H&E staining. The pathological features of these tissues were observed in detail with a scanning microscope (Pannoramic MIDI II, provided by 3DHISTECH China) and the related changes were recorded. Microscopic images of representative histological sections demonstrated synovial hyperplasia (S), pannus formation (P), significant infiltration of inflammatory cells (I), destruction of bone tissue (B), and cartilage injury (C).

2.9. Immunohistochemical (IHC) staining

IHC staining used PV-6000 universal 2-step immunohistochemistry (Zsbio, China), following the experimental instructions. The tissue sections were permeabilized for 15 min, with antigen retrieval for 15 min and endogenous peroxidase activity blocking for 10 min, and serum blocking for 15 min. The primary antibody was then added and incubated for 12 h at 4 °C. The next day, a biotin-labeled secondary antibody was incubated for 20 min, and then treated with horseradish peroxidase streptavidin solution. After rinsing with PBS, color development was achieved using

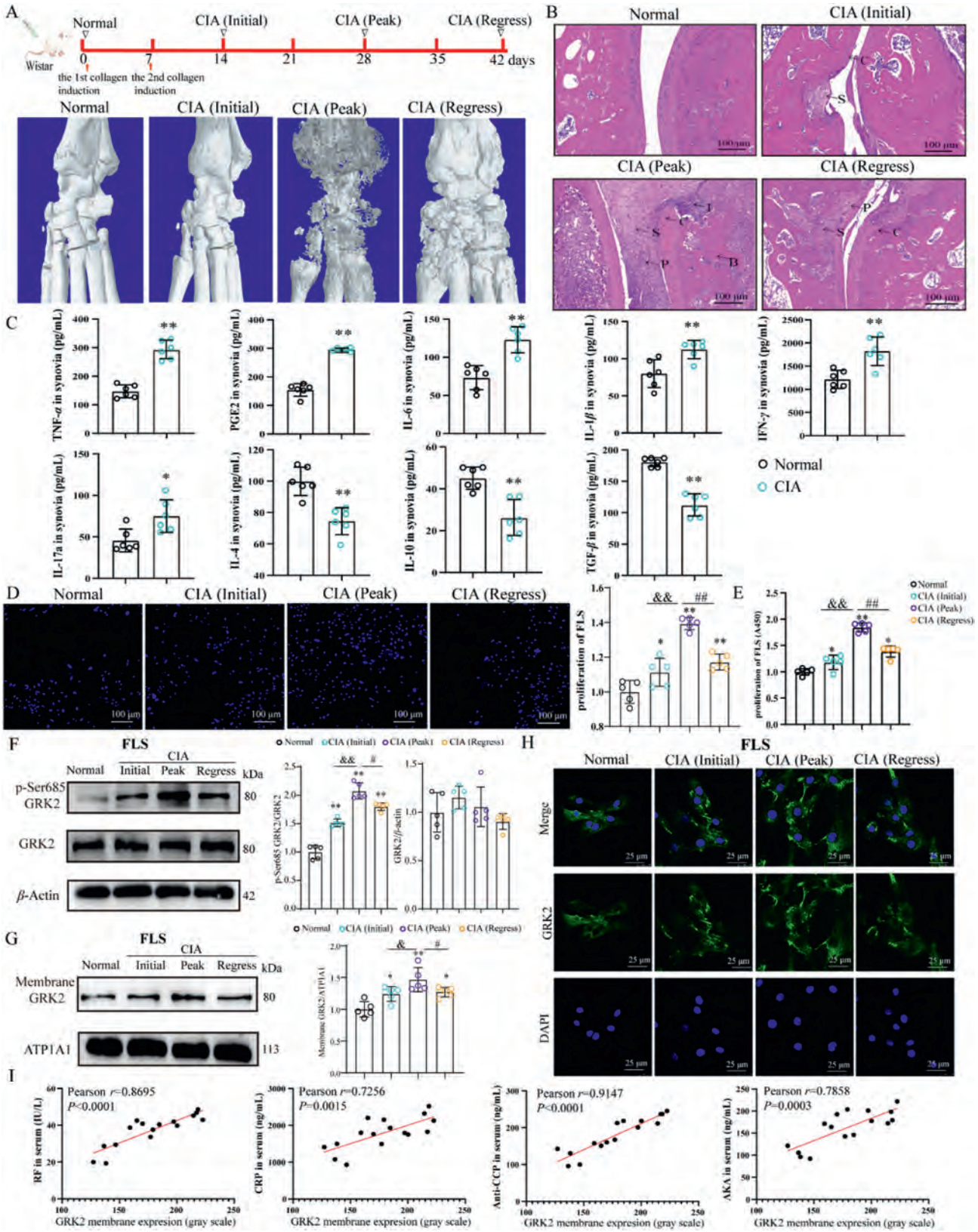

Figure 2 Membrane expression of GRK2 in FLSs of CIA rats. (A) Bone destruction of the ankle joint (front) in different inflammatory stages of CIA rats was measured by micro-CT ($n = 3$). (B) Ankle joint in different inflammatory stages of CIA rats was measured by H&E staining ($n = 5$, scale bar = 100 μm). (C) ELISA quantified pro-inflammatory and anti-inflammatory cytokines in the synovia of CIA rats ($n = 6$, one-way ANOVA, $^{*}P < 0.05$, $^{**}P < 0.01$ *vs*. normal group). (D) High-content cell imager captured cell images to count cell number [$n = 6$, scale bar = 100 μm, one-way ANOVA, $^{*}P < 0.05$, $^{**}P < 0.01$ *vs*. normal group; $^{\&\&}P < 0.01$ *vs*. CIA (Initial) group; $^{\#\#}P < 0.01$ *vs*. CIA (Peak)

DBA, followed by hematoxylin staining. The results were finally examined using a scanning microscope (Pannoramic MIDI II, 3DHISTECH, China).

2.10. Micro-computed tomography (Micro-CT)

The ankle joints of the rats were fixed and then subjected to micro-CT scanning (SkyScan 1276, Bruker, Germany), using an 85 kV voltage and a 200 μA ray tube current, with a scanning angle of 180°. 3D reconstruction with NRecon software (v1.7.4.2) was used to process the original images. The regions of interest were subsequently analysed using Analyser software (v1.20.3.0).

2.11. X-ray fluoroscopic imaging system

The ankle joints were placed in the animal X-ray irradiator (LabScope, Glenbrook Technologies, USA) under the following conditions, X-ray tube emission voltage: 0−25 KV; X-ray tube focus: 10 μm, 5 W power; image resolution 15 lp/mm; the radiation dose from 5 cm distance was less than 5 μSv/h (25 KV); outside the radiation tube, the radiation dose was less than 0.5 μSv/h. Swelling in joint soft tissue, joint deformation, and joint space were observed.

2.12. Ultrasonic testing

Before ultrasonography, each rat was anesthetized with 2% isoflurane, and hair around the knee joint was removed, and then a coupling agent was added. *In vitro* ultrasound imaging was conducted using B mode, and color Doppler functions (Vevo 2100, VisualSonics, Canada), using an 18 MHz transducer. Changes in echogenic signals were recorded.

2.13. Confocal immunofluorescence

FLSs were incubated for 12 h at 4 °C with a 1:100 dilution of rabbit anti-GRK2 antibody, and then anti-rabbit Alexa Fluor 488 (1:100) was incubated for 1 h at 37 °C. The cell membrane was stained with PlasMem Bright Red working solution for 5 min, and the cell nucleus was stained with DAPI solution for 3 min, followed by four rinses with PBS. A confocal microscope (Leica SP8, Germany) captured fluorescent images.

2.14. Co-immunoprecipitation (Co-IP) and Western blot

The cells were lysed in lysis buffer with HEPES (25 mmol/L), EDTA (5 mmol/L), NaCl (150 mmol/L), 1% Triton X-100, 10% glycerol, and protease and phosphatase inhibitors, for 30 min on ice. The supernatant lysates were obtained by centrifugation. To preclear the lysates, normal mouse IgG (sc-2025, Santa Cruz Biotechnology, USA) was added and incubated for 2 h at 4 °C. After this, FLAG, MYC, GRK2, or TRAF2 antibodies were introduced for immunoprecipitation, along with protein A/G binding agarose beads, and incubated for 12−16 h at 4 °C. The immunoprecipitates were eluted with 5 × SDS buffer, and immunoblotting with the specified antibodies.

2.15. Biochemical markers and serum or synovia cytokines detection

Following the kit's operating guidelines, the concentrations of rheumatoid factor (RF), C-reactive protein (CRP), anti-keratin antibody (AKA), and anti-cyclic citrullinated peptide antibody (anti-CCP) in serum samples were measured by ELISA. They also measured levels of a range of inflammatory and immunomodulatory factors in serum and synovial tissue. These include PGE2, TNF-α, IL-6, IL-1β, IL-17a, IFN-γ, IL-4, IL-10, and TGF-β.

2.16. Quantitative PCR (qPCR)

The total RNA of cells was obtained by TRIzol reagent (Invitrogen, 15596018). RNA samples were used to perform reverse transcription with MonScript RTase III reagent kit (Monad, MR00201) and PCR amplification tests with MonScript ChemoHS qPCR Mix (Monad, MQ00401). The design primers are shown in Supporting Information Table S2. The internal reference gene was GAPDH, and the $2^{-\Delta\Delta CT}$ method analysed the relative expression of the gene.

2.17. RNA-sequencing (RNA-seq)

ST samples from both normal and CIA rats were subjected to high-throughput transcriptome sequencing using an Illumina HiSeq2500 instrument at Majorbio Co., Ltd. (China) to identify genes that are abnormally and specifically expressed. Reactome enrichment analysis was conducted to assess the functional implications of the dysregulated genes in the ST of CIA rats. The sequencing and analysis followed the standard RNA-seq protocol as outlined by DEGseq.

2.18. His-GRK2 pull-down assay

After transfecting the cells, cells were lysed in lysis buffer for 20−30 min. The supernatant lysates were obtained by centrifugation. Lysates containing His-tagged proteins were then incubated with Ni Sepharose beads HP (Cytiva, USA) for 2 h at 4 °C. The lysates were mixed with the Ni beads bound to His-tagged proteins and incubated for 12 h at 4 °C. The protein−bead complexes were washed with lysis buffer. Western blot analysis was performed to visualize the pull-down bands.

group]. (E) CCK-8 analysis indicated cell proliferation activity across groups [$n = 6$, one-way ANOVA, $^{*}P < 0.05$, $^{**}P < 0.01$ *vs*. normal group; $^{\&\&}P < 0.01$ *vs*. CIA (Initial) group; $^{\#\#}P < 0.01$ *vs*. CIA (Peak) group]. (F) Western blotting detected *p*-Ser685 GRK2 and total GRK2 protein levels in FLSs of CIA rats [$n = 5$, one-way ANOVA, $^{**}P < 0.01$ *vs*. normal group, $^{\&\&}P < 0.01$ *vs*. CIA (Initial) group; $^{\#}P < 0.05$ *vs*. CIA (Peak) group]. (G) Membrane protein extraction and Western blot analysis confirmed GRK2 membrane expression in FLSs of CIA rats [$n = 5$, one-way ANOVA, $^{*}P < 0.05$, $^{**}P < 0.01$ *vs*. normal group, $^{\&}P < 0.05$ *vs*. CIA (Initial) group; $^{\#}P < 0.05$ *vs*. CIA (Peak) group]. (H) Confocal microscopy illustrated GRK2 intracellular localization in CIA rat FLSs ($n = 5$, scale bar = 25 μm). (I) Correlation analysis showed significant relationships between GRK2 membrane expression and RF ($n = 5$, Pearson coefficient analysis, $r = 0.8695$, $P < 0.0001$), CRP ($n = 5$, Pearson coefficient analysis, $r = 0.7259$, $P = 0.0015$), anti-CCP ($n = 5$, Pearson correlation analysis, $r = 0.9147$, $P < 0.0001$) and AKA ($n = 5$, Pearson correlation analysis, $r = 0.7858$, $P = 0.0003$). All data are presented as mean ± SD.

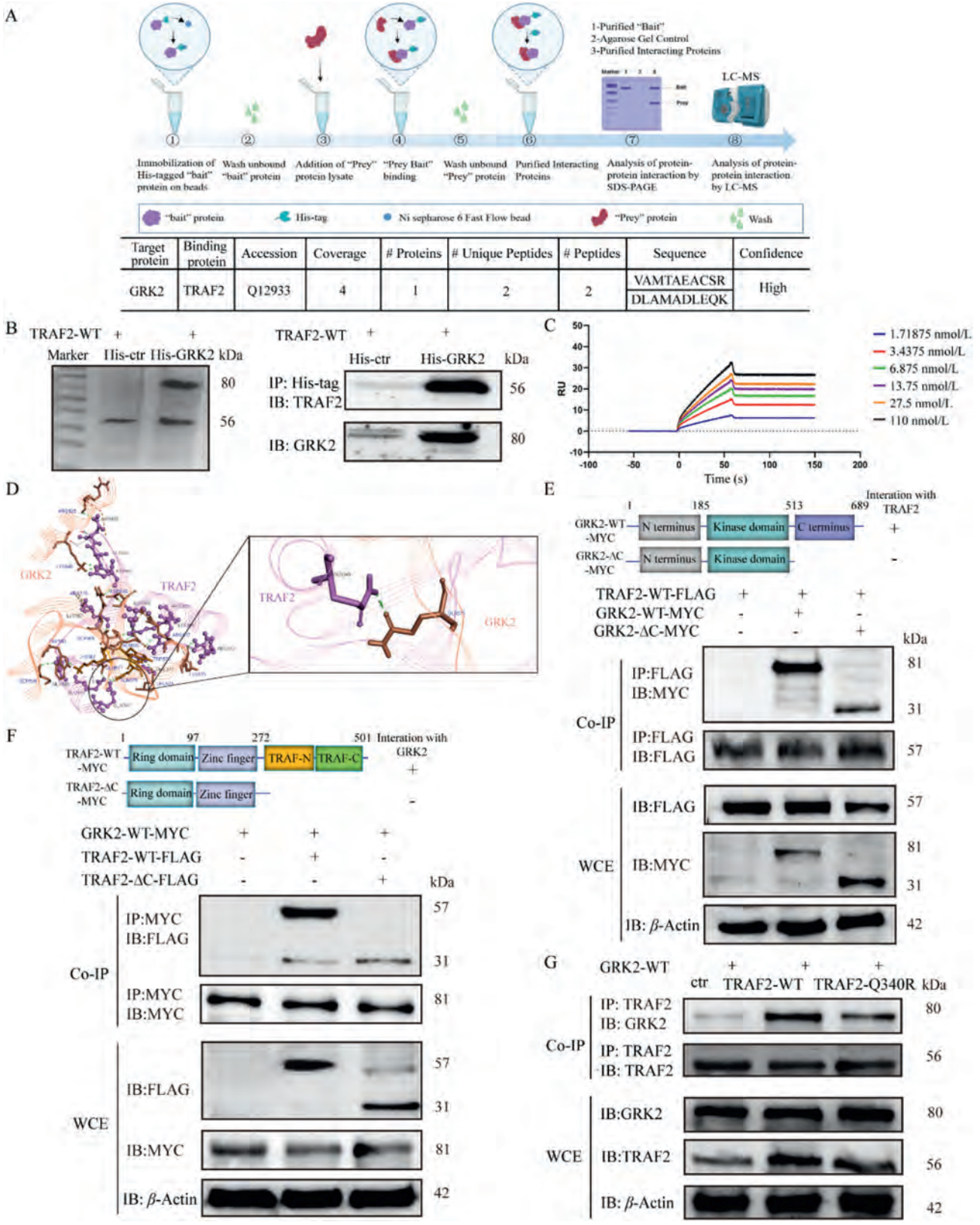

Target protein	Binding protein	Accession	Coverage	# Proteins	# Unique Peptides	# Peptides	Sequence	Confidence
GRK2	TRAF2	Q12933	4	1	2	2	VAMTAEACSR DLAMADLEQK	High

Figure 3 GRK2 binds to Gln340 residue in the C-terminus of TRAF2. (A) TRAF2 proteins (296-VAMTAEACSR-305 and 332-DLAMADLEQK-341) interacting with GRK2 from MS analysis of peptides pulled down using Ni beads in FLS. (B) Direct binding of GRK2-His and TRAF2 using the His pull-down assay. The pull-down bands were detected by Coomassie brilliant blue staining (left) and Western blot (right) (n = 3). (C) SPR was performed using human recombinant GRK2 full-length and TRAF2 full-length proteins. The response−concentration curve was used to evaluate K_d value. (D) Docking between GRK2 and TRAF2. The figure shows that GRK2 formed

2.19. Label-free quantification protein assay

The human His-GRK2 protein was incubated with Ni-Sepharose HP beads and then combined with lysates from MH7A cells at 4 °C overnight. The protein complex bound to the Ni beads was eluted using a protein elution buffer and subsequently analysed using mass spectrometry (MS) (Q Exactive HFX Orbitrap, ThermoFisher Scientific, USA). Raw MS files were processed on a Linux OS server (Debian 9) using MaxQuant software. The UniProt FASTA databases and contaminant database were used to search MS spectra. Quantification was based on the MS1 peak area and maxLFQ, with all other parameters set to default. Proteins and peptides matching the database were analysed.

2.20. SPR

Recombinant GRK2 (50 μg/mL) was immobilized on the CM5 sensor chip. TRAF2 protein solutions were prepared in a series of concentrations (1.71875, 3.4375, 6.875, 13.75, 27.5, and 110 nmol/L) and flowed for 150 s during each run (rate of 10 μL/min). BIAcore T200 Control software (v.2.0, GE Healthcare, USA) recorded data from the sample and corrected the values. BIAcore T200 Evaluation software determined the association and dissociation constants (K_d). Finally, Origin 7 software exported the data to generate the final figures.

2.21. Molecular docking modelling

To confirm the binding sites and examine the binding mode, the ZDOCK program in Discovery Studio (DS) 2020 Client (Accelrys Software Inc., USA) was used. ZDOCK employs rigid-body docking of two molecules. This was followed by refinement using RDOCK. The protein structures of human GRK2 and TRAF2 were sourced from the AlphaFold Protein Structure Database.

2.22. Statistical analysis

The experimental data are based on at least three independent replicates, and the results are presented in the form of mean followed by standard deviation (SD) to ensure the reliability and accuracy of the results. For statistical analysis, we adopted the professional software GraphPad Prism (v8.3.0) for processing. For the comparison between the two groups of data, we used Student's *t*-test to evaluate the significance of the difference. When comparing more than two sets of data, one-way analysis of variance (ANOVA) was used to comprehensively examine the differences between the groups. In addition, Pearson correlation analysis was used to explore the linear relationship between variables. In all statistical tests, $P < 0.05$ represents a significant difference.

3. Results

3.1. Expression and intracellular localization of GRK2 in patients with RA

GRK2 has an N-terminal domain, a kinase domain, and a C-terminal domain, but the role of GRK2 in the regulation of FLS hyperproliferation requires further study. To this end, we first detected GRK2 expression in ST of RA patients and normal individuals. Elevated GRK2 protein levels were confirmed in ST of RA patients compared to normal controls by IHC staining (Fig. 1A). To characterise GRK2 expression in FLSs, we isolated FLSs from ST of patients with RA and normal individuals. High-content cell imager and CCK-8 proliferation assays both demonstrated the proliferation of FLSs in RA patients increased (Fig. 1B and C). Then, we compared GRK2 expression and intracellular localization in FLSs. Interestingly, our results suggested that the expression of GRK2 mRNA and protein in FLSs of patients with RA was not significantly altered compared to their counterparts from normal individuals (Fig. 1D; Supporting Information Fig. S1A and S1B), whereas Ser685 phosphorylation of GRK2 and GRK2 membrane expression was increased in FLSs (Fig. 1D−F). We further examined the expression and intracellular of GRK2 in peripheral blood mononuclear cells (PBMCs) of RA patients; increased GRK2 transmembrane activity in PBMCs of RA patients was consistent with that in FLSs (Fig. S1B−S1E). Moreover, in RA FLSs, GRK2 membrane expression was positively correlated with RF and CRP levels (Fig. 1G), suggesting that the translocation of GRK2 to the cell membrane may play a vital role in the clinicopathology of patients with RA.

3.2. Membrane-bound GRK2 levels correlate with the development of synovial hyperplasia and inflammation

RA is a chronic progressive disease. To explore the expression and intracellular localization of GRK2 during the different stages of RA, CIA animal models were established. We first examined clinical indexes and serological biomarkers of CIA rats and observed that the clinical indexes (the global assessment, arthritis index, swollen joint count, and paw swelling of the secondary side of the joint) were significantly higher during the peak of inflammation compared to normal rats or to rats during the early stage and remission stage of CIA (Supporting Information Fig. S2A and S2B). Serological biomarkers, including RF and anti-CCP, were also significantly higher during the peak of inflammation as well as were positively correlated with levels of TNF-α, PGE2, IL-6, IL-1β, IFN-γ, and IL-17a, and negatively correlated with levels of IL-4, IL-10, and TGF-β in serum (Fig. S2C−S2E).

conventional hydrogen bond with TRAF2 at Gln340, Glu344, Glu346, Lys357, Asp360, Arg363, Lys364, Arg372, Phe377, Asn438, Gln437, Glu479, and Asp487. Arg, arginine; Asn, asparagine; Asp, aspartate; Glu, glutamate; Gln, glutamine; Lys, lysine; Phe, phenylalanine. (E) TRAF2 binds to the GRK2 C-terminus. Schematic of domain structures of GRK2 deletion mutants interaction with TRAF2 full-length (up); co-IP of FLAG-tagged TRAF2 constructs with MYC-tagged GRK2 full length (amino acids 1−689) and GRK2 deletion mutants (amino acids 1−513) in HEK293 cells is shown (below) ($n = 3$). WCE, whole-cell extracts. (F) GRK2 bound to the TRAF2 C-terminus. Schematic of domain structures of TRAF2 deletion mutants interaction with GRK2 full-length (up); co-IP of MYC-tagged GRK2 constructs with FLAG-tagged TRAF2 full-length (amino acids 1−501) and TRAF2 deletion mutants (amino acids 1−272) in HEK293 cells is shown (below) ($n = 3$). (G) TRAF2 Gln340 was a key amino acid residue in the GRK2 interaction ($n = 3$).

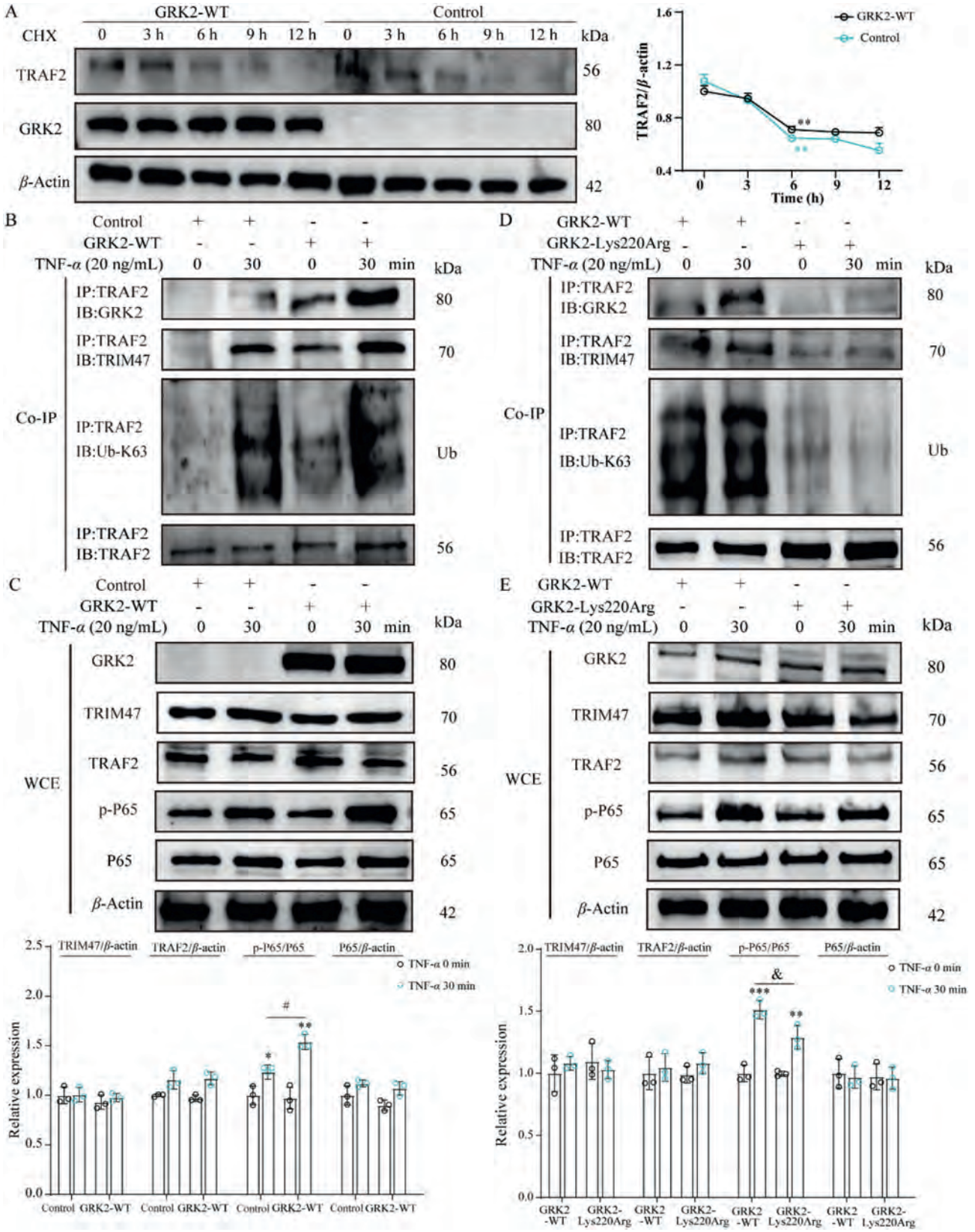

Figure 4 GRK2 mediates Lys63-linked polyubiquitination of TRAF2 depending on its kinase activity. (A) HEK293 cells transfected with MYC-tagged GRK2-WT and EV plasmids were incubated with CHX (100 μg/mL) for 3, 6, 9, and 12 h. Immunoblotting was performed with specific antibodies to evaluate the stability and degradation of TRAF2 ($n = 3$, one-way ANOVA, $^{**}P < 0.01$ *vs*. CHX 3 h). (B, D) HEK293 cells expressing either GRK2-WT or the kinase-dead mutant GRK2-Lys220Arg were stimulated with 20 ng/mL TNF-α for 30 min. Western blot analysed the levels of total GRK2, TRIM47, TRAF2, P65, and phosphorylated P65 ($n = 3$). (C, E) After TNF-α stimulation, HEK293 cell lysates underwent immunoprecipitation with anti-TRAF2. Immunoblotting

Applying micro-CT to quantify the changes in bone destruction, we found that bone damage of the ankle joint in CIA rats at the peak of inflammation was more severe than that in the early-stage group (Fig. 2A; Supporting Information Fig. S3A). We also used H&E staining and ultrasound assays, which showed that the synovial hyperplasia, joint destruction, and neovascularisation at the peak of inflammation of CIA rats were more severe than those of normal rats or CIA rats during the early stage or remission stage (Fig. 2B; Fig. S3B and S3C). Next, we performed RNA-seq of ST of normal and CIA rats to evaluate potential alterations in gene expression that could alter signal transduction. Reactome enrichment analysis showed that multifarious inflammatory-associated pathways, including GPCR, TNF, and Toll-like signalling pathways, were changed in CIA compared to normal rats, implying that these signalling pathways were abnormally activated at the peak of inflammation (Fig. S3D). In addition, the expression of pro-inflammatory cytokines (TNF-α, PGE2, IL-6, IL-1β, IFN-γ, and IL-17a) in synovial fluid (SF) from CIA rats were all upregulated; the expression of anti-inflammatory cytokines (IL-4, IL-10, and TGF-β) in SF from CIA rats were all downregulated (Fig. 2C); and FLSs proliferation of CIA rats was significantly increased, especially at the peak of inflammation of CIA (Fig. 2D and E). We further determined that the mRNA and protein expression of GRK2 in FLSs of CIA rats were not different from that of controls, but phosphorylation of GRK2 (Fig. 2F; Supporting Information Fig. S4A) and GRK2 membrane expression (Fig. 2G and H) in FLSs of CIA rats were increased, especially at the peak of inflammation, which was similar to our findings in clinical specimens. Similarly, GRK2 transmembrane activity was increased in PBMCs and spleen cells of CIA rats (Fig. S4B−S4D). Pearson's correlation test showed that GRK2 membrane expression was positively correlated with RF, CRP, AKA, and anti-CCP levels (Fig. 2I). Together, these results demonstrate that higher GRK2 membrane expression may predict the aggravation of arthritis, indicating that increased GRK2 membrane translocation might play a role in RA progression.

3.3. The GRK2 C-terminus interacts with Gln340 on TRAF2 C-terminus

GRK2 is a key signalling protein, impacting various biological processes, such as cell proliferation and inflammation, *via* its interactions with all kinds of substrate proteins[28]. To investigate the potential interacting partners of GRK2 through which it may promote FLS hyperproliferation, we stably expressed and purified GRK2-His in HEK293 cells and performed immunoprecipitation (IP) experiments on purified GRK2-His protein and RA FLSs (MH7A cells) lysates (Supporting Information Fig. S5A). Subsequent MS analysis identified TRAF2 as a candidate GRK2-binding protein, and specifically that GRK2 bound to residues Val296−Arg305 and Asp332−Lys341 of the C-terminal domain of TRAF2 (Fig. 3A; Fig. S5B). The IP assay also found that GRK2 interacted with GIT1, HSP90, CDK2, P53, and NF-κB1, which was consistent with previously reported results[29] (Fig. S5C). We biochemically confirmed the interaction between GRK2 and TRAF2 by performing a pull-down assay using His-GRK2 and Sepharose 6FF beads exposed to HEK293 cells lysates overexpressing the gene encoding for TRAF2 (Fig. 3B). We then used purified recombinant proteins to demonstrate GRK2−TRAF2 interaction by SPR experiments, revealing K_d values of 31.2 nmol/L (Fig. 3C) indicative of stable binding. We also performed molecular docking simulations of GRK2 and TRAF2 crystal structures to predict the modes of their interaction, finding that the C-terminal domain of GRK2 formed extensive hydrogen bonding interactions with residues Gln340, Glu344, Glu346, Lys357, Asp360, Arg363, Lys364, Arg372, Phe377, Asn438, Gln437, Glu479, and Asp487 of the C-terminal domain of TRAF2 (Fig. 3D). Combined with the IP−MS, these results demonstrate direct binding between GRK2 and TRAF2 and suggest that TRAF2 Gln340 may be a key residue for GRK2−TRAF2 interaction.

To determine which GRK2 domain mediates the GRK2−TRAF2 binding, we transiently co-transfected vectors expressing MYC-tagged GRK2 without the C-terminal domain (GRK2-ΔC; comprising amino acids 1−513) along with full-length MYC-tagged GRK2 and FLAG-tagged TRAF2 into HEK293 cells. The first round of IP analysis of the cell lysate was performed with anti-FLAG antibody, followed by the second round of Western blot detection with anti-MYC antibody. Although full-length GRK2 bound to TRAF2, GRK2-ΔC failed to bind TRAF2 (Fig. 3E), suggesting that the C-terminal GRK2 domain is responsible for TRAF2 binding. Similarly, TRAF2 also contains several conserved domains, contributing to protein−protein interactions[30]. Therefore, to determine which domain of TRAF2 is required for the GRK2 association, we co-expressed a FLAG-tagged truncated TRAF2 protein missing the C-terminal domain (TRAF2-ΔC, comprising amino acids 1−272) with FLAG-tagged full-length TRAF2 and MYC-GRK2. IP and immunoblotting analysis showed that only the full-length TRAF2 could pull down GRK2 (Fig. 3F), indicating that GRK2 binds to TRAF2 *via* its C-terminal domain. Finally, we engineered a TRAF2 Gln340Arg mutant and evaluated the binding of this construct or wild-type (WT) TRAF2 with GRK2. IP and immunoblot analysis showed that Gln340 was required for TRAF2 binding (Fig. 3G). Taken together, our results demonstrate direct binding of the C-terminal domains of GRK2 and TRAF2, with Gln340 in TRAF2 serving as an essential residue for this interaction.

3.4. GRK2−TRAF2 interaction promotes TRAF2 Lys63 polyubiquitination and NF-κB activation

To determine the effect of GRK2 on TRAF2 expression and activity, we first investigated whether GRK2 affects TRAF2 protein expression by treating cells with protein synthesis inhibitor cycloheximide (CHX). HEK293 cells were transfected with GRK2-WT plasmids, or empty vector (EV), as control. TRAF2 protein levels began to gradually decline at 6 h in both the control group and the GRK2 group (Fig. 4A), indicating that GRK2 binding does not affect TRAF2 protein expression. TRAF2 is an important adaptor molecule in TNFR signalling, promoting downstream signalling cascades, such as NF-κB activation. In general, TRAF2 polyubiquitylation on Lys48 induces protein degradation, whereas Lys63 polyubiquitylation modulates TRAF2

was subsequently conducted with anti-GRK2, anti-TRIM47, anti-K63-linked ubiquitin, and anti-TRAF2 antibodies ($n = 3$, one-way ANOVA, $^{*}P < 0.05$, $^{**}P < 0.01$, $^{***}P < 0.001$ *vs*. TNF-α 0 min; $^{\#}P < 0.05$ *vs*. control group; $^{\&}P < 0.05$ *vs*. GRK2 WT group). All data are presented as mean ± SD.

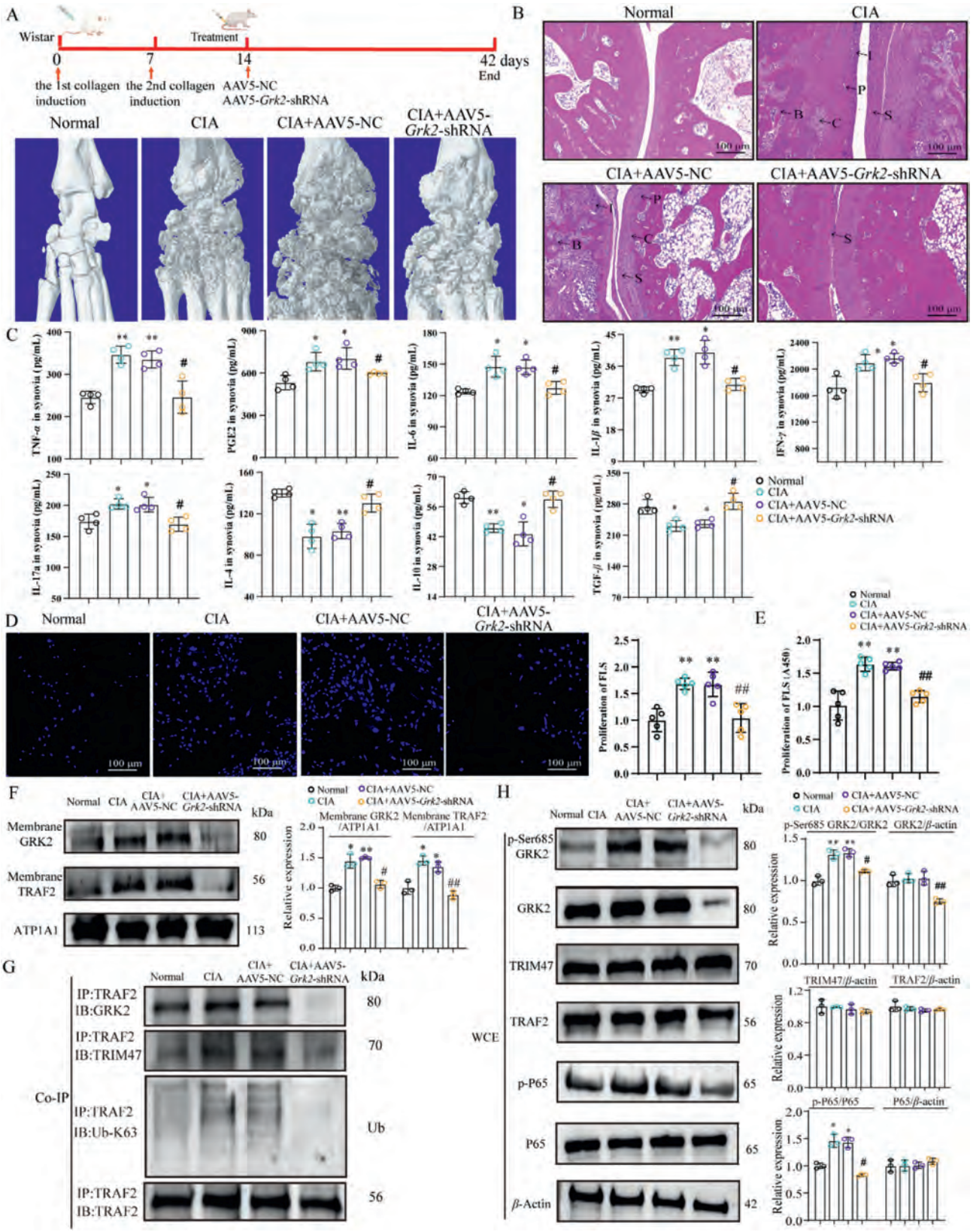

Figure 5 Knockdown of GRK2 improves synovial hyperplasia of CIA *in vivo* and *in vitro*. (A) Rats were used to establish a CIA model for 2 weeks, and then joints of rats were injected with AAV5-NC or *Grk2*-shRNA immediately after CIA, and the rats were euthanized at 3 weeks. GRK2 knockdown alleviated joint destruction of CIA (front) by micro-CT analyses ($n = 3$). (B) H&E staining revealed that GRK2 knockdown significantly reduced overall pathological damage in the ankle joints of CIA rats ($n = 5$, scale bar = 100 μm). (C) The effect of GRK2 knockdown on cytokines expression in SF of CIA rats ($n = 4$, one-way ANOVA, $^{*}P < 0.05$, $^{**}P < 0.01$ *vs*. normal group; $^{\#}P < 0.05$ *vs*.

activity, often leading to signalling activation and trafficking[31]. It was reported that TRIM47 mediated the activation of NF-κB possibly by increasing ubiquitylation of TRAF2 Lys63[32], prompting us to hypothesise that GRK2 binding to TRAF2 might recruit TRIM47-mediated polyubiquitylation of TRAF2 Lys63, thereby activating NF-κB signalling to trigger FLS hyperproliferation. To test this, GRK2-WT plasmids or EV plasmids were transfected into HEK293 cells, and then the cells were stimulated with TNF-α, followed by IP and Western blot. We found that GRK2 strongly promoted interaction between TRAF2 and TRIM47 as well as mediated TRAF2 Lys63 polyubiquitylation (Fig. 4B). Furthermore, GRK2-WT promotes TNF-α-dependent NF-κB transcriptional activation, as shown by increased phosphorylation of P65 (Fig. 4C), again supporting the notion that the GRK2−TRAF2 interaction promotes NF-κB activation *via* TRAF2 polyubiquitylation. We next repeated the aforementioned experiment with the kinase-deficient GRK2 Lys220Arg mutant, which showed that TNF-α-induced GRK2−TRAF2 interactions were decreased in the presence of GRK2-Lys220Arg compared to GRK2-WT; as anticipated, GRK2-Lys220Arg also resulted in downregulated TRIM47 recruitment, TRAF2 Lys63 polyubiquitylation, and NF-κB activation (Fig. 4D and E). Taken together, these data support that regulation of TRAF2 Lys63 polyubiquitylation by GRK2 is strictly dependent on GRK2 kinase activity.

3.5. GRK2 knockdown decreases GRK2−TRAF2 interactions and improves synovial hyperplasia in CIA rats

Because our data indicate that GRK2 binds to TRAF2 and promotes its activation, we wondered whether GRK2 might play a role in RA progression. We specifically posited that decreased GRK2−TRAF2 interactions may inhibit the proliferation of FLSs in CIA rats. To examine this, we initiated an experiment in the knee joints of CIA rats using the AAV5 vector carrying *Grk2* short hairpin RNA (shRNA) or non-targeting control shRNA (NC) construct for the total *Grk2* knockdown. Knockdown efficiency of *Grk2* in FLSs was confirmed by Western blot (Supporting Information Fig. S6A) and qPCR (Fig. S6B), suggesting that *Grk2*-shRNA1 strongly downregulated GRK2 expression in FLSs of rats *in vitro*. Successful transduction of GFP with AAV5 vector into knee joints of rats was determined using a fluorescence microscope (Fig. S6C), indicating that AAV5 could infect FLSs of the knee joint *in vivo* by injecting into the knee joint cavity, and *in vivo* RNAi silencing of the *Grk2* gene was achieved by AAV5 delivery of *Grk2*-shRNA. AAV5-*Grk2*-shRNA was injected into the knee joint cavities of rats, with all joint tissues collected 28 days after AAV5 injection to analyze on-target silencing efficiency and the pathological features of the synovium. qPCR results showed that AAV5-*Grk2*-shRNA1 markedly downregulated GRK2 mRNA levels in FLSs of ST *in vivo* compared to the AAV5-NC group (Fig. S6D). We found that, compared to the AAV5-NC group, GRK2 knockdown in ST of CIA rats resulted in decreased scores on clinical indexes (Supporting Information Fig. S7A and S7B), decreased serological biomarkers of arthritis, decreased serum pro-inflammatory factors, and increased serum anti-inflammatory factors levels (Fig. S7C). GRK2 knockdown also significantly alleviated bone damage of the ankle joint (Fig. 5A; Supporting Information Fig. S8A and S8B) and inhibited synovial hyperplasia of the knee joint, ankle joint, and ST in CIA rats (Fig. 5B; Fig. S8C). In addition, in the SF of CIA rats, GRK2 knockdown reduced pro-inflammatory cytokines and increased anti-inflammatory cytokines levels (Fig. 5C).

To investigate the regulatory role of GRK2 knockdown on primary FLSs proliferation and TRAF2−NF-κB signalling, we performed proliferation assays on FLSs isolated from CIA rats. GRK2 knockdown cells had FLS proliferation levels similar to FLSs from normal animals and significantly lower than those from CIA rats or CIA rats treated with a control vector (Fig. 5D and E). GRK2 knockdown downregulated GRK2 membrane expression, and decreased the recruitment of TRAF2 to the cell membrane (Fig. 5F). IP and immunoblot analyses demonstrated that GRK2 knockdown significantly downregulated the association of GRK2 with TRAF2, thereby decreasing TRIM47 recruitment and TRAF2 Lys63 polyubiquitylation (Fig. 5G). Moreover, GRK2 knockdown significantly inhibited GRK2 Ser685 phosphorylation and NF-κB activation in FLSs of CIA rats (Fig. 5H). Collectively, our data support a role for the decreased GRK2−TRAF2 interaction in inhibiting proliferation of FLSs in ST in a pathological animal model.

3.6. Decreased GRK2 translocation to the membrane suppresses synovial hyperplasia in vitro and in vivo

GRK2 is a vital Ser/Thr kinase, and, in our study, increased GRK2 membrane localization was positively correlated with abnormal proliferation of FLSs. Some studies indicated that TRAF2 rapidly initiates NF-κB signalling by forming membrane complexes with TNFR and kinase proteins[33,34]. To gain a deeper understanding of the mechanism through which GRK2 modulates synovial hyperplasia, we first studied the effects of exogenous stimuli (PGE2 and TNF-α) on MH7A hyperproliferation and GRK2 expression. MH7A hyperproliferation was significantly upregulated by PGE2 and TNF-α (Supporting Information Fig. S9A−S9C), and 30 min of exposure to PGE2 combined with TNF-α significantly pro-

CIA + AAV5-NC group). (D) FLSs were isolated from Normal, CIA, CIA + AAV5-NC, and CIA + AAV5-*Grk2*-shRNA groups. High-content cell imager captured cell images to count cell number ($n = 5$, scale bar = 100 μm, one-way ANOVA, $^{**}P < 0.01$ *vs*. normal group; $^{\#\#}P < 0.01$ *vs*. CIA + AAV5-NC group). (E) CCK-8 analysis indicated cell proliferation activity across groups ($n = 5$, one-way ANOVA, $^{**}P < 0.01$ *vs*. normal group; $^{\#\#}P < 0.01$ *vs*. CIA + AAV5-NC group). (F) Membrane expression levels of GRK2 and TRAF2 in FLSs were analysed using a membrane protein extraction kit and Western blotting ($n = 3$, one-way ANOVA, $^{*}P < 0.05$, $^{**}P < 0.01$ *vs*. normal group; $^{\#}P < 0.05$, $^{\#\#}P < 0.01$ *vs*. CIA + AAV5-NC group). (G) FLSs were cultured for 48 h. The first round of IP analysis of the cell lysate was performed with anti-TRAF2 antibody, followed by the second round of immunoblotting with anti-GRK2, anti-TRIM47, anti-K63-linked ubiquitin, and anti-TRAF2 ($n = 3$). (H) Western blot analysis of total GRK2, TRIM47, TRAF2, P65, phosphorylated GRK2, and phosphorylated P65 was conducted on lysates from FLSs cultured for 48 h ($n = 3$, one-way ANOVA, $^{*}P < 0.05$, $^{**}P < 0.01$ *vs*. normal group; $^{\#}P < 0.05$, $^{\#\#}P < 0.01$ *vs*. CIA + AAV5-NC group). All data are presented as mean ± SD.

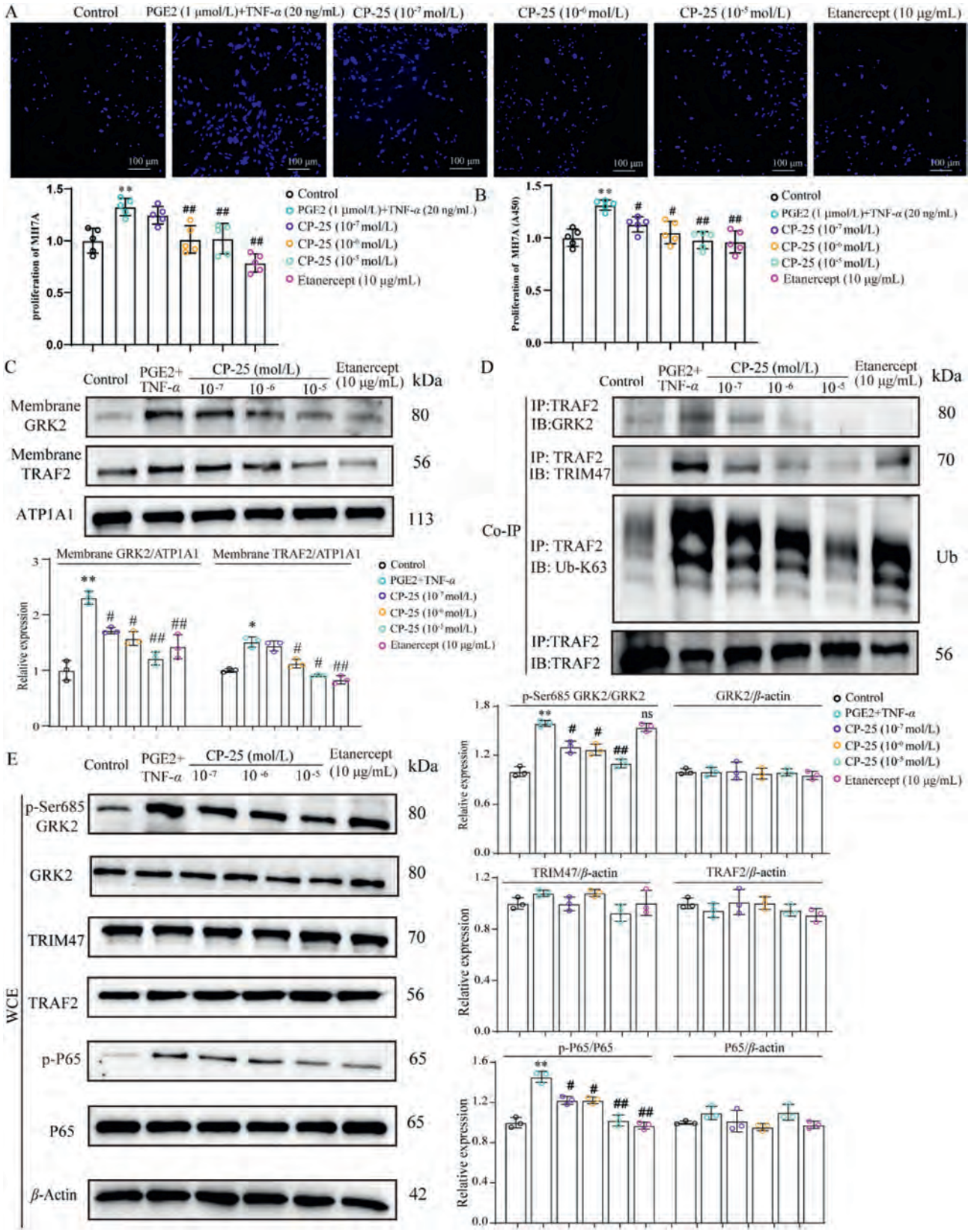

Figure 6 GRK2 activity inhibitor CP-25 improves MH7A abnormal proliferation *in vitro*. (A) MH7A was treated with PGE2 and TNF-α, and exposed to 10^{-7}, 10^{-6}, 10^{-5} mol/L CP-25 for 24 h. High-content cell imager captured cell images to count cell number ($n = 5$, scale bar = 100 μm, one-way ANOVA, $^{**}P < 0.01$ *vs*. control group; $^{\#\#}P < 0.01$ *vs*. PGE2+TNF-α group). (B) CCK-8 analysis indicated cell proliferation activity across groups ($n = 5$, one-way ANOVA, $^{**}P < 0.01$ *vs*. control group; $^{\#}P < 0.05$, $^{\#\#}P < 0.01$ *vs*. PGE2+TNF-α group). (C) GRK2 and TRAF2 membrane expression in MH7A were detected by membrane protein extraction kit and Western blot ($n = 3$, one-way ANOVA,

moted GRK2 transmembrane localization, GRK2 Ser685 phosphorylation and NF-κB activation (Fig. S9D). Both GRK2 activity inhibitor CP-25 and TNF-α inhibitor etanercept significantly attenuated the proliferation of stimulated MH7A cells (Fig. 6A and B). We then isolated membrane proteins from treated MH7A cells and performed immunoblot analysis, which showed that PGE2 and TNF-α stimulation induced GRK2 transmembrane localization and promoted TRAF2 recruitment to the cell membrane and GRK2−TRAF2 complex formation, resulting in TRIM47-mediated polyubiquitylation of TRAF2 Lys63 and NF-κB activation. Further research showed that CP-25 impaired TRAF2 recruitment to the cell membrane, GRK2−TRAF2 complex formation, and TRIM47 recruitment, decreasing TRAF2 Lys63 polyubiquitylation, GRK2 Ser685 phosphorylation and NF-κB activation by downregulating GRK2 transmembrane activity. However, the inhibitory effect of TNF-α inhibitor etanercept was not by affecting the phosphorylation of GRK2 at Ser685, but by down-regulating GRK2−TRAF2 interaction (Fig. 6C−E). This result was consistent with the previous research findings that TNF-α induces the recruitment of TRAF2 on the cell membrane, which is conducive to the binding of TRAF2 to GRK2 and increases GRK2 membrane expression[35]. These results further suggest that GRK2−TRAF2 complex formation and GRK2 transmembrane localization may play a vital role in the abnormal proliferation of FLSs.

To verify the role of membrane-localized GRK2 in synovial hyperplasia *in vivo*, CIA rats were treated with CP-25 or positive control drug etanercept. CP-25 and etanercept treatment decreased clinical and serological biomarkers of arthritis (Supporting Information Fig. S10A and S10B) as well as decreased serum pro-inflammatory cytokines and increased serum anti-inflammatory cytokines levels (Fig. S10C). Both CP-25 and etanercept also significantly inhibited CIA-induced bone damage of the ankle joint (Fig. 7A; Supporting Information Fig. S11A and S11B) and inhibited synovial hyperplasia of the knee joint, ankle joint, and ST (Fig. 7B; Fig. S11C and S11D) compared to control treatment. In addition, in the SF, pro-inflammatory cytokines levels were decreased and anti-inflammatory cytokines levels were increased by CP-25 and etanercept compared to control treatment (Fig. 7C). Finally, in primary FLSs isolated from the knee joint of CIA rats, CP-25 and etanercept treatment both significantly inhibited CIA-induced hyperproliferation (Fig. 7D and E). Consistent with our *in vitro* results, CP-25 decreased the recruitment and association of TRAF2 with GRK2, and inhibited GRK2 phosphorylation and TRAF2−NF-κB activation, consistent with our proposed mechanism of membrane translocation of GRK2 facilitating TRAF2 polyubiquitylation and NF-κB signalling. However, the positive control drug TNF-α inhibitor etanercept also decreased GRK2 and TRAF2 membrane expression, inhibited interactions between TRAF2 and GRK2, and attenuated TRAF2−NF-κB activation, but it did not affect GRK2 Ser685 phosphorylation (Fig. 7F−H). These data indicate that increased GRK2 transmembrane activity promotes the recruitment of TRAF2 to the cell membrane and GRK2−TRAF2 interaction, leading to TRIM47-mediated polyubiquitylation of TRAF2 Lys63 and NF-κB activation, which may be a novel mechanism for GRK2 to regulate FLS hyperproliferation (Fig. 8).

4. Discussion

The inhibition of FLS hyperproliferation is one of the investigative focuses for treating RA. In this study, while confirming its roles in synovial hyperplasia, we revealed that GRK2 transmembrane activity is positively correlated with abnormal proliferation of FLSs and RA progression. Mechanistically, the effect of GRK2 was executed through direct binding with TRAF2 and subsequent recruitment of the E3 ligase TRIM47, which polyubiquitylated TRAF2, resulting in NF-κB activation and FLS hyperproliferation.

GRK2 influences multiple cellular functions related to autoimmune diseases, such as RA[36,37]. In addition to GRK2's typical role of regulating GPCR through phosphorylation-dependent desensitization and internalization, it can also exert effects in a phosphorylation-independent manner by participating in a variety of protein−protein interactions[38,39]. FLSs, macrophages, and endothelial cells are all key cellular components involved in the pathogenesis of RA. Our previous research has demonstrated that GRK2 Ser685 phosphorylation reflects increased GRK2 activity and can promote GRK2 translocation, leading to angiogenesis and FLS hyperproliferation[20,23]. Increased GRK2 transmembrane activity promotes FLS hyperproliferation and macrophage polarization by binding to EP4[21,25]. Therefore, increased transmembrane activity of GRK2 can regulate FLSs, macrophages, and endothelial cell function in RA. In the present study, we found that GRK2 was highly expressed in RA ST, but its total expression in isolated FLSs from RA ST was not significantly different compared to FLSs from normal ST. However, GRK2 membrane expression and GRK2 Ser685 phosphorylation were higher in FLSs from RA patients *versus* normal ST. We also observed that GRK2 was significantly expressed in the cell membranes of PBMCs from patients with RA, and the phosphorylation of GRK2 at Ser685 was significantly increased. Increased GRK2 transmembrane activity promoted RA FLS hyperproliferation. High CRP and RF seropositivity are validated as clinical indices for the diagnosis of RA[27]. In this study, GRK2 translocation activity was positively correlated with CRP and RF levels of RA patients. Accordingly, similar results were observed in FLSs and PBMCs of CIA rats. These results suggest a critical role for membrane-bound GRK2 in regulating FLS functions and inflammation in ST of RA patients and CIA rats.

TNF-α, as a multifunctional pro-inflammatory cytokine, is a critical mediator in the pathogenesis of RA. TRAF2 acts as a critical adaptor molecule that bridges TNF-α signalling from the cell surface receptors to the intracellular machinery, thereby activating NF-κB signaling, mediating cell proliferation, and the production of pro-inflammatory factor[40-42]. Our previous research has discovered that TNF-α induces the recruitment of TRAF2 to the cell membrane, thereby upregulating the binding of TRAF2 to GRK2 and GRK2 membrane expression, leading to FLS proliferation[35]. In addition, it was shown that increased

$^{*}P < 0.05$, $^{**}P < 0.01$ *vs*. control group; $^{\#}P < 0.05$, $^{\#\#}P < 0.01$ *vs*. PGE2+TNF-α group). (D) MH7A was cultured for 48 h. The first round of IP analysis of the cell lysate was performed with anti-TRAF2, followed by the second round of immunoblotting with anti-GRK2, anti-TRIM47, anti-K63-linked ubiquitylation, and anti-TRAF2 ($n = 3$). (E) MH7A was cultured for 48 h. The cell lysates were analysed by Western blot analysis of total GRK2, TRIM47, TRAF2, P65, phosphorylated GRK2, and phosphorylated P65 ($n = 3$, one-way ANOVA, $^{**}P < 0.01$ *vs*. control group; $^{ns}P > 0.05$, $^{\#}P < 0.05$, $^{\#\#}P < 0.01$ *vs*. PGE2+TNF-α group). All data are presented as mean ± SD.

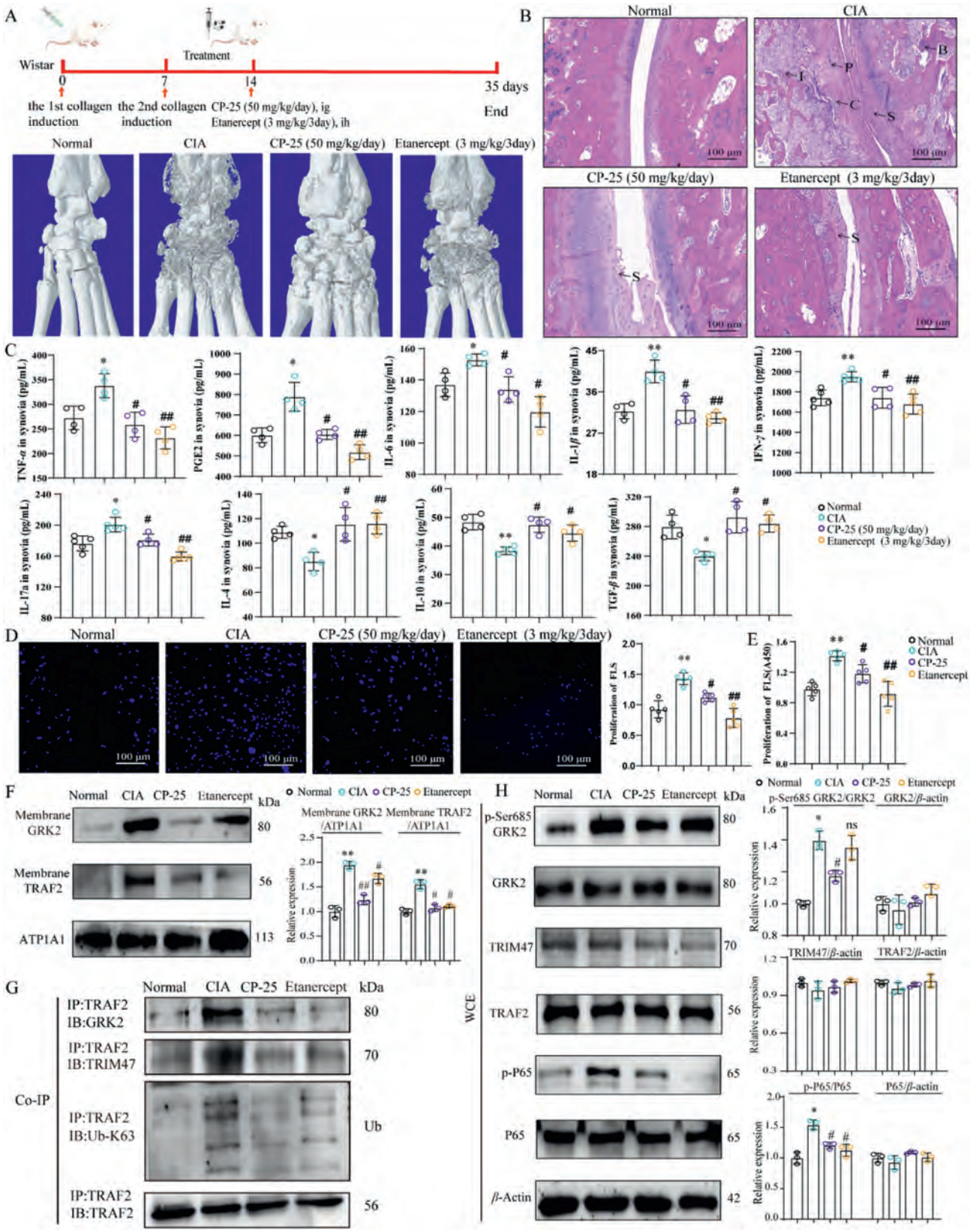

Figure 7 GRK2 activity inhibitor CP-25 improves synovial hyperplasia of CIA *in vivo* and *in vitro*. (A) Rats were used to establish a CIA model for 2 weeks, CP-25 (50 mg/kg/d) was administered by gavage for 3 weeks, and etanercept (3 mg/kg/3d) was given subcutaneously every three days for 3 weeks. CP-25 alleviated joint destruction of CIA by micro-CT analyses ($n = 3$). (B) H&E staining indicated that CP-25 significantly reduced overall pathological damage in the ankle joints of CIA rats ($n = 5$, scale bar = 100 μm). (C) The effect of CP-25 treatment on cytokines expression in the SF of CIA rats ($n = 4$–5, one-way ANOVA, $^{*}P < 0.05$, $^{**}P < 0.01$ *vs*. normal group; $^{\#}P < 0.05$,

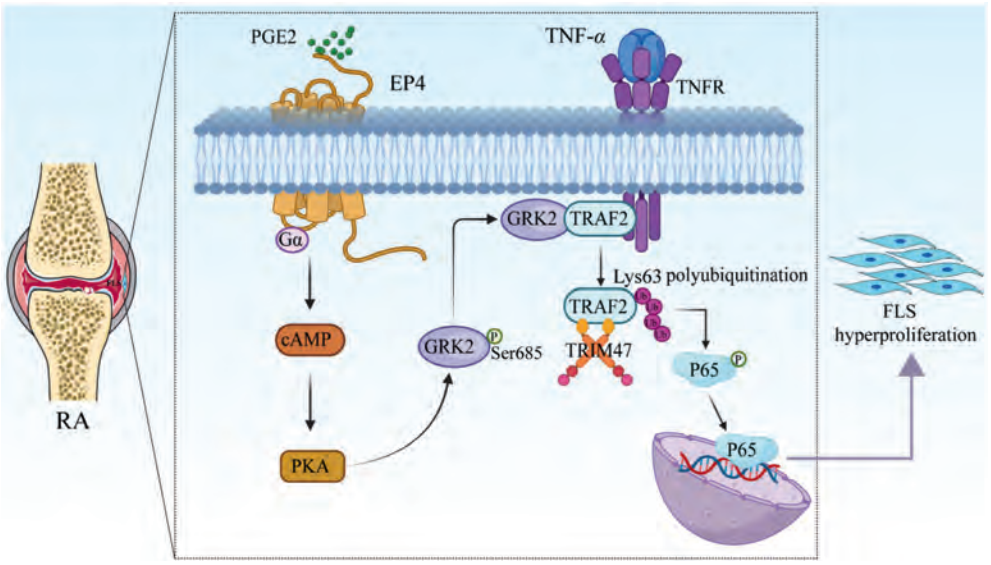

Figure 8 Schematic diagram depicting the mechanism by which activation of GRK2−TRAF2−NF-κB axis promotes hyperproliferation of RA FLSs.

polyubiquitylation of TRAF2 Lys63 in FLSs is associated with the development of RA and that the E3 ligase TRIM47, a key component of the TNF-α signalling pathway, promotes TRAF2 Lys63 polyubiquitylation[32,43]. Although GRK2 and TRAF2 perform different functions at the molecular level, the potential interaction between the two and their regulation of signalling pathways have fueled speculation that they may play a key role in the course of RA. To further characterize this interaction, we investigated FLSs derived from RA patients with the help of advanced bioinformatic analysis. This study revealed the identity of TRAF2 as a novel interacting partner of GRK2, and further indicated that GRK2 could guide TRAF2 to the cell membrane of FLSs, which provided a new perspective for understanding the synergistic role of the two in RA pathology. This led to TRIM47-mediated polyubiquitylation of TRAF2 Lys63 and subsequent activation of NF-κB signalling. We specifically found that the GRK2 C-terminus (amino acids 514−689) mediated the interaction with TRAF2 and was required for NF-κB activation and that TRAF2 Gln340 was also involved in the interaction. We further demonstrated that GRK2 kinase activity (GRK2-Lys220) was required to promote TRAF2 Lys63 polyubiquitylation, suggesting that GRK2 may be important for TRIM47-mediated ubiquitylation of TRAF2. These results provide strong support for a model in which a GRK2−TRAF2−TRIM47−NF-κB axis is a key regulator of synovial hyperplasia.

GRK2 translocation to the membrane of FLSs was significantly induced by PGE2 and TNF-α, indicating that GRK2 might be a sensor in response to stimulation. Exposure of FLSs from CIA rats treated with GRK2 activity inhibitor CP-25 or genetic *GRK2* knockdown decreased GRK2 membrane expression and GRK2 Ser685 phosphorylation, decreased the inflammatory response, and improved synovial hyperplasia both *in vitro* and *in vivo*, indicating that GRK2 subcellular localization in the cell membrane is required for the activity of the GRK2−TRAF2−TRIM47−NF-κB axis. It has been reported that the association of TRAF2 with GRK2 contributes to bringing GRK2 to the cell membrane in response to TNF-α stimulation, promoting EP4 desensitization and production of intracellular cAMP[35]. Etanercept is one of these drugs that is useful for RA treatment. Etanercept inhibits TRAF2 and GRK2 membrane expression, TRAF2−GRK2 association, and NF-κB activation to prevent initiation of FLSs proliferation without affecting the phosphorylation of GRK2 at Ser685 in this study.

5. Conclusions

Our study establishes an innovative pathological mechanism to initiate FLS hyperproliferation and RA progression, with increased GRK2 translocation activity as a major driver of this progression. Clinical studies have shown that in most samples

$^{\#\#}P < 0.01$ *vs*. CIA group). (D) FLSs were isolated from Normal, CIA, CP-25, and Etanercept groups. High-content cell imaging was used to capture images and count cell numbers ($n = 5$, scale bar = 100 μm, one-way ANOVA, $^{**}P < 0.01$ *vs*. normal group; $^{\#}P < 0.05$, $^{\#\#}P < 0.01$ *vs*. CIA group). (E) CCK-8 analysis indicated cell proliferation activity across groups ($n = 5$, one-way ANOVA, $^{**}P < 0.01$ *vs*. normal group; $^{\#}P < 0.05$, $^{\#\#}P < 0.01$ *vs*. CIA group). (F) Membrane expression levels of GRK2 and TRAF2 in FLSs were analysed using a membrane protein extraction kit and Western blotting ($n = 3$, one-way ANOVA, $^{**}P < 0.01$ *vs*. normal group; $^{\#}P < 0.05$, $^{\#\#}P < 0.01$ *vs*. CIA group). (G) FLSs were cultured for 48 h. The first round of IP analysis of the cell lysate was performed with anti-TRAF2, followed by the second round of immunoblotting with anti-GRK2, anti-TRIM47, anti-K63-linked ubiquitylation, and anti-TRAF2 ($n = 3$). (H) Western blot analysis of total GRK2, TRIM47, TRAF2, P65, phosphorylated GRK2, and phosphorylated P65 was conducted on lysates from FLSs cultured for 48 h ($n = 3$, one-way ANOVA, $^{*}P < 0.05$ *vs*. normal group; $^{ns}P > 0.05$, $^{\#}P < 0.05$ *vs*. CIA group). All data are presented as mean ± SD.

from patients with RA, the translocation activity of GRK2 shows a significant trend of enhancement and is positively correlated with several serological RA biomarkers, further confirming its importance in the pathological process of RA. These findings encourage further study of the role of the GRK2 transmembrane activity in the pathogenesis of RA to develop novel therapeutic strategies.

Acknowledgements

We thank the staff at Majorbio for performing RNA sequencing and data analyzing, Biotree for performing MS data analyzing and Topscience for performing SPR. We also thank the affected patients and healthy volunteers in this study. Graphical abstract was created with BioRender.com. This research was supported by National Natural Science Foundation of China (Nos. 82104187, 82173824, and 82430114), Natural Science Foundation of Anhui Province (No. 2108085QH382, China), Project funded by China Postdoctoral Science Foundation (Nos. 2021T140002 and 2021M700184), the Postdoctoral Science Foundation of Anhui Province (No. 2020B430, China), Postgraduate Innovation Research and Practice Program of Anhui Medical University (No. YJS20230162, China).

Author contributions

Chenchen Han: Data curation, Formal analysis, Writing-Original draft preparation, Writing-Reviewing and Editing, Funding acquisition. Wei Wei: Conceptualization, Methodology, Writing-Reviewing and Editing, Funding acquisition. Yang Ma: Supervision. Liang Xu: Resources. Liping Jiang, Weikang Wang, Shujun Zuo: Visualization, Investigation. Jintao Gu, Luying Chen, Zhuo Chen, Jiajie Kuai, Xuezhi Yang: Visualization.

Conflicts of interest

The authors declare no conflicts of interest.

Appendix A. Supporting information

Supporting information to this article can be found online at https://doi.org/10.1016/j.apsb.2025.02.031.

References

1. Conrad N, Misra S, Verbakel JY, Verbeke G, Molenberghs G, Taylor PN, et al. Incidence, prevalence, and co-occurrence of autoimmune disorders over time and by age, sex, and socioeconomic status: a population-based cohort study of 22 million individuals in the UK. *Lancet* 2023;**401**:1878−90.
2. Carmona-Rivera C, Carlucci PM, Moore E, Lingampalli N, Uchtenhagen H, James E, et al. Synovial fibroblast-neutrophil interactions promote pathogenic adaptive immunity in rheumatoid arthritis. *Sci Immunol* 2017;**2**:eaag3358.
3. Nygaard G, Firestein GS. Restoring synovial homeostasis in rheumatoid arthritis by targeting fibroblast-like synoviocytes. *Nat Rev Rheumatol* 2020;**16**:316−33.
4. Kugler M, Dellinger M, Kartnig F. Cytokine-directed cellular crosstalk imprints synovial pathotypes in rheumatoid arthritis. *Ann Rheum Dis* 2023;**82**:1142−52.
5. Tu J, Chen W, Fang Y, Han D, Chen Y, Jiang H, et al. PU.1 promotes development of rheumatoid arthritis *via* repressing FLT3 in macrophages and fibroblast-like synoviocytes. *Ann Rheum Dis* 2023;**82**:198−211.
6. Evron T, Daigle TL, Caron MG. GRK2: multiple roles beyond G protein-coupled receptor desensitization. *Trends Pharmacol Sci* 2012;**33**:154−64.
7. Tesmer VM, Kawano T, Shankaranarayanan A, Kozasa T, Tesmer JJ. Snapshot of activated G proteins at the membrane: the Gαq−GRK2−Gβγ complex. *Science* 2005;**310**:1686−90.
8. Yang X, Zhang W, Wang L, Zhao Y, Wei W. Metabolite-sensing GPCRs in rheumatoid arthritis. *Trends Pharmacol Sci* 2024;**45**:118−33.
9. Crudden C, Shibano T, Song D, Dragomir MP, Cismas S, Serly J, et al. Inhibition of G protein-coupled receptor kinase 2 promotes unbiased downregulation of IGF1 receptor and restrains malignant cell growth. *Cancer Res* 2021;**81**:501−14.
10. Jiang X, Yang P, Ma L. Kinase activity-independent regulation of cyclin pathway by GRK2 is essential for zebrafish early development. *Proc Natl Acad Sci U S A* 2009;**106**:10183−8.
11. Degos V, Peineau S, Nijboer C, Kaindl AM, Sigaut S, Favrais G, et al. G protein-coupled receptor kinase 2 and group I metabotropic glutamate receptors mediate inflammation-induced sensitization to excitotoxic neurodegeneration. *Ann Neurol* 2013;**73**:667−78.
12. Beautrait A, Michalski KR, Lopez TS, Mannix KM, McDonald DJ, Cutter AR, et al. Mapping the putative G protein-coupled receptor (GPCR) docking site on GPCR kinase 2: insights from intact cell phosphorylation and recruitment assays. *J Biol Chem* 2014;**289**:25262−75.
13. Echeverría E, Velez Rueda AJ, Cabrera M, Juritz E, Burghi V, Fabián L, et al. Identification of inhibitors of the RGS homology domain of GRK2 by docking-based virtual screening. *Life Sci* 2019;**239**:116872.
14. Zhao Z, Lee RTH. An essential role for Grk2 in Hedgehog signalling downstream of Smoothened. *EMBO Rep* 2021;**22**:e52895.
15. Bliziotes M, Gunness M, Zhang X, Nissenson R, Wiren K. Reduced G-protein-coupled-receptor kinase 2 activity results in impairment of osteoblast function. *Bone* 2000;**27**:367−73.
16. Sterne-Marr R, Leahey PA, Bresee JE, Dickson HM, Ho W, Ragusa MJ, et al. GRK2 activation by receptors: role of the kinase large lobe and carboxyl-terminal tail. *Biochemistry* 2009;**48**:4285−93.
17. Lee IH, Song SH, Campbell CR, Kumar S, Cook DI, Dinudom A. Regulation of the epithelial Na^+ channel by the RH domain of G protein-coupled receptor kinase, GRK2, and Galphaq/11. *J Biol Chem* 2011;**286**:19259−69.
18. Brackley AD, Sarrami S, Gomez R, Guerrero KA, Jeske NA. Identification of a signaling cascade that maintains constitutive δ-opioid receptor incompetence in peripheral sensory neurons. *J Biol Chem* 2017;**292**:8762−72.
19. Yang X, Zhao Y, Wei Q, Zhu X, Wang L, Zhang W, et al. GRK2 inhibits Flt-1^+ macrophage infiltration and its proangiogenic properties in rheumatoid arthritis. *Acta Pharm Sin B* 2024;**14**:241−55.
20. Guo P, Jiang J, Chu R, He F, Ge M, Fang R, et al. GRK2 mediated degradation of SAV1 initiates hyperplasia of fibroblast-like synoviocytes in rheumatoid arthritis. *Acta Pharm Sin B* 2024;**14**:1222−40.
21. Han C, Li Y, Zhang Y, Wang Y, Cui D, Luo T, et al. Targeted inhibition of GRK2 kinase domain by CP-25 to reverse fibroblast-like synoviocytes dysfunction and improve collagen-induced arthritis in rats. *Acta Pharm Sin B* 2021;**11**:1835−52.
22. Wang X, Tu J, Jiang J. Angiotensin II type 2 receptor modulates synovial macrophage polarization by inhibiting GRK2 membrane translocation in a rat model of collagen-induced arthritis. *J Immunol* 2020;**205**:3141−53.
23. Han CC, Liu Q, Zhang Y, Li YF, Cui DQ, Luo TT, et al. CP-25 inhibits PGE2-induced angiogenesis by down-regulating EP4/AC/cAMP/PKA-mediated GRK2 translocation. *Clin Sci* 2020;**134**:331−47.
24. Hong ZY, Tie QS, Zhang LL. Targeted inhibition of the GRK2/HIF-1α pathway is an effective strategy to alleviate synovial hypoxia and inflammation. *Int Immunopharmacol* 2022;**113**:109271.
25. Yang X, Li S, Zhao Y, Li S, Zhao T, Tai Y, et al. GRK2 mediated abnormal transduction of PGE2−EP4−cAMP−CREB signaling

induces the imbalance of macrophages polarization in collagen-induced arthritis mice. *Cells* 2019;**8**:1596.
26. Jia XY, Chang Y, Wei F, Dai X, Wu YJ, Sun XJ, et al. CP-25 reverses prostaglandin E4 receptor desensitization-induced fibroblast-like synoviocyte dysfunction *via* the G protein-coupled receptor kinase 2 in autoimmune arthritis. *Acta Pharmacol Sin* 2019;**40**:1029−39.
27. Aletaha D, Neogi T, Silman AJ, Funovits J, Felson DT, Bingham 3rd CO, et al. 2010 rheumatoid arthritis classification criteria: an American College of Rheumatology/European League against Rheumatism collaborative initiative. *Ann Rheum Dis* 2010; **69**:1580−8.
28. Cheng H, Guo P, Su T, Jiang C, Zhu Z, Wei W, et al. G protein-coupled receptor kinase type 2 and β-arrestin2: key players in immune cell functions and inflammation. *Cell Signal* 2022;**95**: 110337.
29. Ferrero KM, Koch WJ. GRK2 in cardiovascular disease and its potential as a therapeutic target. *J Mol Cell Cardiol* 2022;**172**:14−23.
30. Park YC, Ye H, Hsia C, Segal D, Rich RL, Liou HC, et al. A novel mechanism of TRAF signaling revealed by structural and functional analyses of the TRADD−TRAF2 interaction. *Cell* 2000;**101**:777−87.
31. Li S, Wang D, Zhao J, Weathington NM, Shang D, Zhao Y. The deubiquitinating enzyme USP48 stabilizes TRAF2 and reduces E-cadherin-mediated adherens junctions. *FASEB J* 2018;**32**:230−42.
32. Qian Y, Wang Z, Lin H, Lei T, Zhou Z, Huang W, et al. TRIM47 is a novel endothelial activation factor that aggravates lipopolysaccharide-induced acute lung injury in mice *via* K63-linked ubiquitination of TRAF2. *Signal Transduct Target Ther* 2022;**7**:148.
33. Sangaré LO, Yang N, Konstantinou EK, Lu D, Mukhopadhyay D, Young LH, et al. Toxoplasma GRA15 activates the NF-κB pathway through interactions with TNF receptor-associated factors. *mBio* 2019; **10**:e00808-19.
34. Wu W, Wang J, Xiao C, Su Z, Su H, Zhong W, et al. SMYD2-mediated TRAF2 methylation promotes the NF-κB signaling pathways in inflammatory diseases. *Clin Transl Med* 2021;**11**:e591.
35. Tai Y, Huang B, Guo PP, Wang Z, Zhou ZW, Wang MM, et al. TNF-α impairs EP4 signaling through the association of TRAF2−GRK2 in primary fibroblast-like synoviocytes. *Acta Pharmacol Sin* 2022;**43**: 401−16.
36. Pfleger J, Gresham K, Koch WJ. G protein-coupled receptor kinases as therapeutic targets in the heart. *Nat Rev Cardiol* 2019;**16**:612−22.
37. Guccione M, Ettari R, Taliani S, Da Settimo F, Zappalà M, Grasso S. G-protein-coupled receptor kinase 2 (GRK2) inhibitors: current trends and future perspectives. *J Med Chem* 2016;**59**:9277−94.
38. Xiang G, Acosta-Ruiz A. Control of $G\alpha_q$ signaling dynamics and GPCR cross-talk by GRKs. *Sci Adv* 2022;**8**:eabq3363.
39. Duan J, Liu H, Zhao F, Yuan Q, Ji Y, Cai X, et al. GPCR activation and GRK2 assembly by a biased intracellular agonist. *Nature* 2023;**620**: 676−81.
40. Loh C, Park S, Lee A, Yuan R, Ivashkiv LB, Kalliolias GD. TNF-induced inflammatory genes escape repression in fibroblast-like synoviocytes: transcriptomic and epigenomic analysis. *Ann Rheum Dis* 2019;**78**:1205−14.
41. Zhang LL, Xiao H, Zhang F, Wu YJ, Shu JL, Li Y, et al. BAFF, involved in B cell activation through the NF-κB pathway, is related to disease activity and bone destruction in rheumatoid arthritis. *Acta Pharmacol Sin* 2021;**42**:1665−75.
42. Potter C, Eyre S, Cope A, Worthington J, Barton A. Investigation of association between the TRAF family genes and RA susceptibility. *Ann Rheum Dis* 2007;**66**:1322−6.
43. Sun H, Li S, Xu Z, Liu C, Gong P, Deng Q. SNHG15 is a negative regulator of inflammation by mediating TRAF2 ubiquitination in stroke-induced immunosuppression. *J Neuroinflammation* 2022;**19**:1.